

From Data Deluge to Data Curation: A Filtering-WoRA Paradigm for Efficient Text-based Person Search

Jintao Sun
Beijing Institute of Technology
Beijing, China
3120215524@bit.edu.cn

Zhedong Zheng*
Faculty of Science and Technology,
Institute of Collaborative Innovation
University of Macau
Macau, China
zhedongzheng@um.edu.mo

Gangyi Ding
Beijing Institute of Technology
Beijing, China
dgy@bit.edu.cn

ABSTRACT

In text-based person search endeavors, data generation has emerged as a prevailing practice, addressing concerns over privacy preservation and the arduous task of manual annotation. Although the number of synthesized data can be infinite in theory, the scientific conundrum persists that how much generated data optimally fuels subsequent model training. We observe that only a subset of the data in these constructed datasets plays a decisive role. Therefore, we introduce a new Filtering-WoRA paradigm, which contains a filtering algorithm to identify this crucial data subset and WoRA (Weighted Low-Rank Adaptation) learning strategy for light fine-tuning. The filtering algorithm is based on the cross-modality relevance to remove the lots of coarse matching synthesis pairs. As the number of data decreases, we do not need to fine-tune the entire model. Therefore, we propose a WoRA learning strategy to efficiently update a minimal portion of model parameters. WoRA streamlines the learning process, enabling heightened efficiency in extracting knowledge from fewer, yet potent, data instances. Extensive experimentation validates the efficacy of pretraining, where our model achieves advanced and efficient retrieval performance on challenging real-world benchmarks. Notably, on the CUHK-PEDES dataset, we have achieved a competitive mAP of 67.02% while reducing model training time by 19.82%.

CCS CONCEPTS

• **Information systems** → **Retrieval efficiency; Retrieval effectiveness; Multimedia and multimodal retrieval.**

KEYWORDS

Text-based Person Search, Data-centric Learning, Low-Rank Adaptation, Visual-language Pre-training

*Corresponding authors.

Permission to make digital or hard copies of all or part of this work for personal or classroom use is granted without fee provided that copies are not made or distributed for profit or commercial advantage and that copies bear this notice and the full citation on the first page. Copyrights for components of this work owned by others than ACM must be honored. Abstracting with credit is permitted. To copy otherwise, or republish, to post on servers or to redistribute to lists, requires prior specific permission and/or a fee. Request permissions from permissions@acm.org.

ACM Multimedia '24, 28 October 2024 - 1 November 2024, Melbourne, Australia

© 2024 Association for Computing Machinery.
ACM ISBN 978-x-xxxx-xxxx-x/YY/MM... \$15.00
<https://doi.org/10.1145/nnnnnnn.nnnnnnn>

Model Performance Comparison

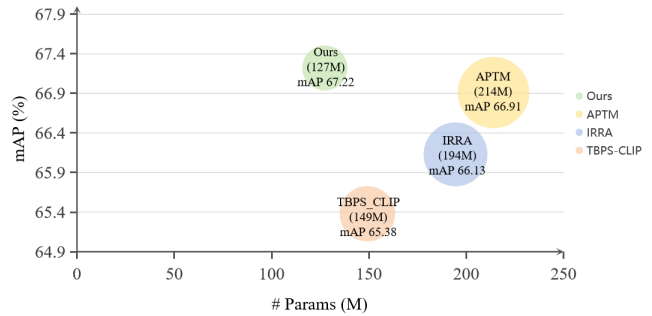


Figure 1: Comparison between the proposed method and existing approaches in terms of mAP accuracy and the parameter numbers. We observe that our method deploys fewer parameters while achieving a higher mAP than competitive methods, i.e., APTM [68], IRRA [23] and TBPS-CLIP [4].

1 INTRODUCTION

Compared to traditional image-based person search [53, 59, 60, 68, 79], which seeks to retrieve target individuals from a vast array of footage or images across different locations and times, text-based person search locates interested individuals from a pool of candidates based on pedestrian descriptions [33]. Given that pedestrian image queries may not be available, text-guided person search emerges as an alternative method. The key lies in mining the fine-grained information from images and texts, blending the complexity of natural language processing with the subtle nuances of visual recognition, and establishing their correspondence. By leveraging the ability to understand complex human descriptions and accurately identify and retrieve images of individuals from a camera system, it can be applied to broad applications in public safety domains such as missing person searches, and rescue operations.

As the sub-task of vision-language retrieval, text-based person search models usually require extensive data for training, but the number of pedestrian data is limited. Most datasets [12, 34, 68, 79] are constructed from three sources. (1) The first source is through sampling from camera footage, accompanied by manual annotations. However, constructing large-scale datasets is often infeasible due to privacy concerns and high costs. (2) The second source involves collecting images and short videos from the internet. Despite expanding dataset sizes, the noisy web text and the inconsistent quality of task images are generally sub-optimal for fine-grained

vision-language learning. (3) Therefore, most researchers [68] resort to leverage the generative models, *e.g.*, GAN [77] and diffusion [47, 52]. For instance, APTM [68] has introduced 1.51M image-text pairs generated by Stable Diffusion [47], showcasing the potential of training on a large synthesized dataset.

Despite significant progress in learning from large synthesized datasets, a fundamental challenge persists: **how can we efficiently extract knowledge when faced with an effectively infinite amount of data, considering the substantial computational costs incurred during training?** We observe two points: (1) Prior works [68, 75, 77] have shown that performance improvements taper off even when copious amounts of additional generated data are supplied. This implies that not all information within massive synthetic datasets is equally valuable; rather, a carefully selected subset, or coreset, may suffice to capture the essence of the training process. (2) If we only need to learn coreset data, it is not necessary for models to update the entirety of parameter volume to ensure training precision. This realization opens up the possibility of significantly trimming down both training time and model complexity. In essence, our focus shifts towards exploring strategies that enable heightened accuracy with leaner data and a more compact parameter footprint.

To this end, we propose a new Filtering-WoRA paradigm, which contains a novel two-stage data filtration method aimed at identifying the coreset to enhance model performance and a WoRA (Weighted Low-Rank Adaptation) algorithm to optimize the pre-training and fine-tuning models, enabling training with fewer parameters while maintaining model performance and increasing computational speed. Specifically, our process begins with dataset purification, including the synthesized dataset for pre-training and the real-world dataset for fine-tuning. To filter out low-quality image-text pairs, *e.g.*, incomplete descriptive details or blurred image details, we leverage the off-the-shelf large cross-modality model to extract features from both images and texts within the dataset and then calculate the cosine similarity between projected image embeddings and projected text embeddings. This process yields a similarity score for each image-text pair, facilitating the selection of high-quality datasets based on our predetermined threshold. Subsequently, to reduce model parameters and enhance computational speed, we opt to freeze the weights from pre-training, indirectly training some dense layers in the neural network by optimizing rank decomposition matrices that change during the adaptation process. By decomposing pre-training and fine-tuning weights into magnitude and direction, our WoRA method introduces three new dimensions to facilitate the modification of the weight matrix and rank decomposition matrix. This approach allows for learning a minimal amount of parameters while simultaneously boosting model performance (see Figure 1). In summary, our contributions are as follows:

- We introduce a new Filtering-WoRA paradigm for efficient text-based person search, which streamlines learning and improves efficiency through focused data curation and targeted parameter updates. The filtering algorithm targets relevant, high-quality synthesized data by assessing cross-modality relevance, while WoRA (Weighted Low-Rank Adaptation)

enables lightweight fine-tuning of a minimal set of model parameters.

- Extensive experiments on three widely-used benchmarks verify that our method could save 19.82% training time compared with the vanilla baseline, while also achieving competitive 76.37%, 66.65%, 67.90% Recall@1 accuracy on CUHK-PEDES, RSTPReid and ICFG-PEDES, respectively.

2 RELATED WORK

2.1 Vision-Language Pre-training

Current VLP research predominantly bifurcates into coarse-grained and fine-grained methodologies. Coarse-grained approaches employ convolutional networks [21, 22, 24] or visual Transformers [25, 31, 42, 46] to extract and encode holistic image features, thereby constructing vision-language models (VLMs). Techniques such as SOHO [21] propose leveraging a Visual Dictionary (VD) for the extraction of comprehensive yet compact image features, facilitating enhanced cross-modal comprehension. ALBEF [31] introduces a contrastive loss for aligning image and text representations before their fusion through cross-modal attention, fostering more grounded vision-language representation learning. Additionally, it utilizes momentum distillation to augment learning capabilities from noisy network data. Although these holistic image-focused methods are efficient, their performance is generally outpaced by fine-grained approaches. Inspired by advancements in the NLP domain, fine-grained methods [9, 14, 28, 32, 37, 44, 55] employ pre-trained object detectors [2, 51] trained on annotated datasets of common objects, such as COCO [38] and Visual Genome [26]. This enables models to recognize and classify all potential object regions within images, representing them as a collection of object-centered features. For instance, VinVL [71] enhances visual representations for V+L tasks and develops an improved object detection model to provide object-centered image representations. However, this object-centered feature representation struggles to capture relationships between multiple objects across different regions, limiting its effectiveness in encoding multi-granularity visual concepts. Another limitation is the inability of the object detector to recognize uncommon objects not present in the training data.

Recently, novel approaches have emerged to bridge the learning of object-level and image-level alignments. E2E-VLP [66] employs DETR [5] as the object detection module to enhance detection capabilities. KD-VLP [41] relies on external object detectors for object knowledge distillation, facilitating cross-modal alignment learning across different semantic layers. OFA [57] formulates visual-linguistic tasks as a sequence-to-sequence (seq2seq) problem, adhering to instruction-based learning during both pre-training and fine-tuning phases, eliminating the need for extra task-specific layers. Uni-Perceiver [80] constructs a unified perception architecture, using a single Transformer and shared parameters for diverse modes and tasks, employing a non-mixed sampling strategy for stable multi-task learning. X-VLM [69] and X2-VLM [70] propose an integrated model with a flexible modular architecture to simultaneously learn multi-granularity alignment and localization, achieving the capability to learn infinite visual concepts related to various text descriptions. In this work, we leverage the proficient vision-language pre-trained model to filter noisy data.

2.2 Text-Image Person Search

Based on the challenging task of language-based person search, which is a fine-grained, cross-modal retrieval challenge, a significant number of methodologies have been developed in recent years to tackle this issue. Existing approaches can broadly be classified into two categories: those based on cross-modal attention interaction [34, 53, 54, 60] and those without cross-modal attention interaction [8, 12, 59, 68, 76]. Methods leveraging cross-modal attention interaction facilitate cross-modal correspondences between regions and words or phrases through paired inputs and predict image-text pair matching scores via attention mechanisms. This enriches interaction between modalities, bridging the modality gap at the cost of higher computational complexity. For example, Li *et al.*[34] propose a novel recurrent neural network with gated neural attention to improve cross-modal learning. Shao *et al.*[53] propose a multimodal shared dictionary (MSD) to reconstruct visual and textual features while using a set of shared and learnable archetypes as queries. In order to improve the performance of person search, different and semantically consistent features are extracted for the two modes in the feature space with uniform granularity. Conversely, methods without cross-modal attention interaction, through the construction of diverse model structures and objective functions, align representations of the two modalities within a shared feature space. These lightweight models, not reliant on complex cross-modal interactions, are computationally more efficient and have even achieved better results than their attention-based counterparts. Zheng *et al.* [76] build an end-to-end dual-path convolutional network to learn image and text representations to take full advantage of supervision capabilities. However, all the person search methods mentioned above fine-tune the entire network for high accuracy, which inherently slows down the process. In contrast, we propose a method based on cross-modal feature extraction for rapid candidate selection and data ranking scores. This approach aims to mitigate the impact of low-quality text-image pairs while reducing model computational parameters to maintain high efficiency in processing.

2.3 Data-Centric Learning

With the surge in popularity of large language models, an increasing demand for vast datasets for model training has emerged [49, 68–70]. However, open-source datasets constructed for training models in real-world scenarios, such as the MALS dataset [68], may encounter issues like incorrect text descriptions, poor image or text quality, and insufficient feature matching between image-text pairs, all of which can adversely affect model training performance. As the size of datasets expands, it is observed that their quality does not invariably scale in tandem [77]. Frequently, a subset of high-caliber data can attain or even exceed the utility of a voluminous but qualitatively inferior dataset. This phenomenon underscores the paramount importance of meticulously curating high-quality datasets, thereby highlighting the necessity for efficiency and precision in dataset construction. For instance, data selection methods [48, 64] aim to identify and train only with the most relevant and informative examples, discarding irrelevant or redundant data. This leads to more efficient learning and improved model performance, especially when dealing with large datasets. Active learning seeks

to reduce labeling costs by selecting the most informative instances for annotation. Data cleaning and preprocessing techniques aim to remove noise, errors, and inconsistencies from the data, making it more suitable for learning. Coreset selection [29, 30] focuses on identifying a small subset of data points (a core set) sufficient for training a model that performs well across the entire dataset. By selecting a representative subset, coreset selection can reduce the computational costs of training and improve model generalization. Our approach advocates for a coreset method aimed at enhancing model performance, proposing the use of the off-the-shelf visual-language models to segment and filter the dataset for text and image pair matching scores, thereby obtaining a coreset dataset for effective training.

3 METHOD

In this section, we first re-introduce the baseline structure, then outline our data filtering strategy, followed by a detailed presentation of our WoRA method for efficiently reducing the model parameters. The brief architecture of our Filtering-WoRA is shown in Figure 2.

3.1 Baseline Revisit

We employ the joint Attribute Prompt Learning and Text Matching Learning framework, APTM [68], as our baseline model. This framework is divided into two main phases: pre-training on the synthesized dataset and fine-tuning on the downstream datasets. The baseline comprises three encoders—image encoder, text encoder, and cross encoder—along with two MLPs-based headers. We do not pursue the network contribution in this work. Therefore, we adopt the common backbone for a fair comparison. The image encoder is a Swin Transformer (Swin-B) [42], while we apply Bert [11] for text encoding. The [CLS] embedding represents the entirety of the image / text. The cross encoder integrates image and text representations for prediction tasks, leveraging the latter 6 layers of Bert to process the previously obtained text and image embeddings, thereby discerning their semantic relationship. We adopt two types of loss functions to bolster alignment constraints, tailored for both image-text and image-attribute associations. The image-text functions encompass Image-Text Contrastive Learning (ITC), Image-Text Matching Learning (ITM), and Masked Language Modeling (MLM), while Attribute Prompt Learning contains Image-Attribute Contrastive Learning (IAC) loss, Image-Attribute Matching Learning (IAM) Loss, and Masked Attribute Modeling (MAM) Loss. The overall APL loss is $\mathcal{L}_{APL} = \frac{1}{3} (\mathcal{L}_{iac} + \mathcal{L}_{iam} + \mathcal{L}_{mam})$, and the full pre-training loss is formulated as: $\mathcal{L}_{total} = \mathcal{L}_{itc} + \mathcal{L}_{itm} + \mathcal{L}_{mlm} + \eta \mathcal{L}_{APL}$, where η is empirically set as 0.8 following [68].

3.2 Data Filtering

As highlighted in our introduction, the acquisition of images is challenged by high annotation costs and concerns over individual privacy and security, necessitating the generation of a large volume of image-text pairs (I, T) through diffusion models, complemented by text descriptions generated by large language models [68]. Despite the potential for achieving high accuracy through extensive pretraining on such data, it becomes apparent that not all generated data are equally effective, with a significant portion being redundant. Additionally, these synthesized datasets often include

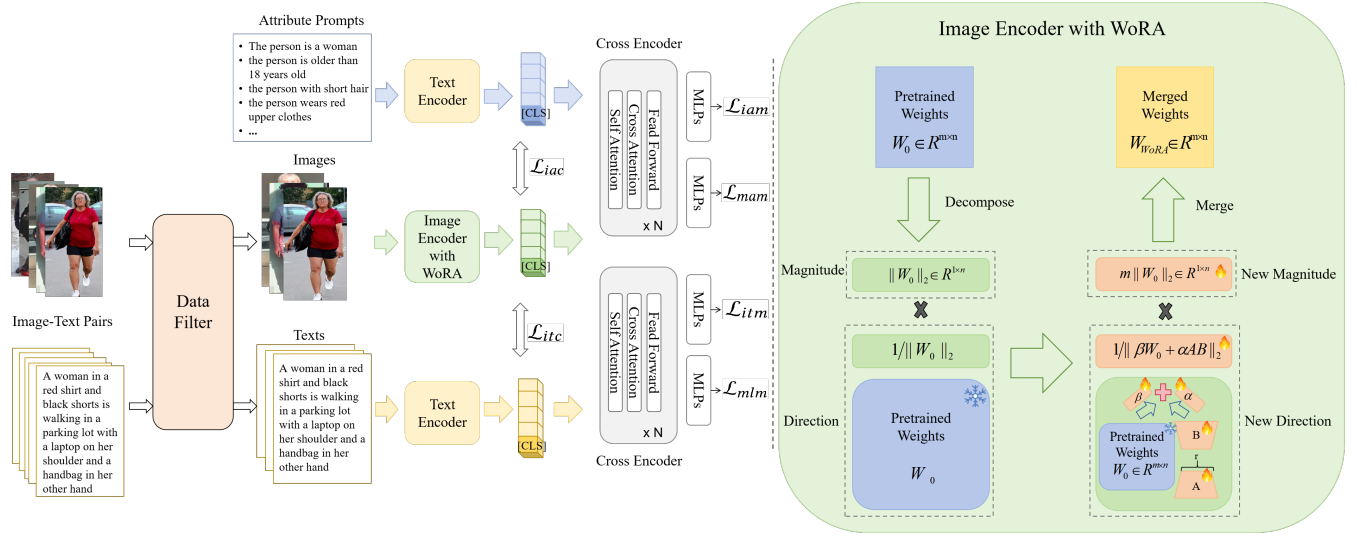


Figure 2: An overview of our architecture. The left half of the picture is the flow chart of the entire training phase. By embedding the image text pair and attribute features, the corresponding features will be obtained through image encoder, text encoder and cross encoder. There are six loss objectives of both text-image and attribute-image matching tasks in the training process. To the right, we present an in-depth illustration of WoRA methodology, meticulously applied within the context of an image encoder. The model is updated by fine-tuning the decomposition of the pre-trained weights into amplitude and direction components and updating both components using LoRA [20] while adding the α and β learnable parameters. Since the image encoder consumes most GPU memory and time. In practice, we mainly apply the WoRA on the image encoder.

noise in the form of image-text pairs with poor matching quality, which can inadequately represent the visual content of images. Such pairs serve as suboptimal signals for learning fine-grained visual-language alignment, potentially disrupting model training. This observation led us to ponder whether reducing the volume of data, focusing solely on a core set, could suffice for model training. Consequently, we devised a data filtering solution a data filtering approach based on the off-the-shelf large cross-modality model, e.g., BLIP-2 [29], leveraging its efficient multimodal feature extraction capabilities to isolate features from both text and images (see Figure 3). We intend to find the appropriate filtering methodology and thresholds to isolate a high-quality core set.

Our method is executed in two phases, starting with the filtering of the synthesized dataset, i.e., MALS, used for pretraining the model. Initially, all image-text pairs (I_M, T_M) within the dataset are processed. Given an image-text pair, the large cross-modality model, i.e., BLIP-2, is employed to extract the corresponding image feature f_{I_M} and text feature f_{T_M} . Subsequently, the training set captions from the real-world downstream dataset, i.e., CUHK-PEDES, acting as validation and interfering texts T_C , are utilized. For each pair, we calculate the cosine similarity between projected image embeddings and projected text embeddings to ascertain their self-similarity Sim_{self} . Simultaneously, the interference similarity Sim_{other} is determined by calculating the similarity between the image feature f_{I_M} and a randomly selected subset of 10,000 validation and interference texts T_C . The following is the formula for calculating the similarity:

$$Sim_{self} = \cos(f_{I_M}, f_{T_M}), Sim_{other} = \cos(f_{I_M}, f_{T_C}), \quad (1)$$

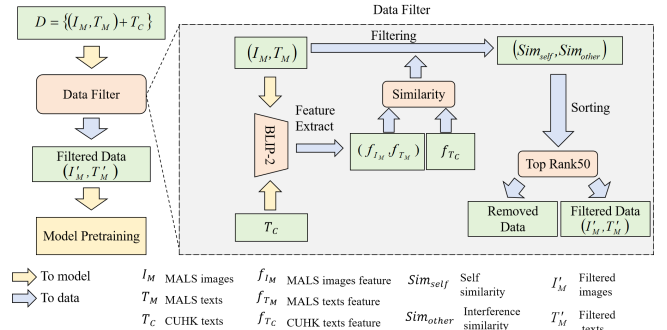


Figure 3: An overview of our data filtering process. We introduced our data filtering process by first entering image text pairs (I, T) and validation and interfering texts T_C are extracted using Blip-2 [29] for feature extraction and then similarity calculation, and sorted according to similarity to get the final filtered data set.

where $\cos(\cdot)$ denotes the cosine similarity. After computing these two types of similarities for all image-text pairs within the training dataset, and then we sort texts according to the similarity from highest to lowest, we set a ranking threshold as 50. It means that an image-text pair is retained only if its self-similarity ranks within the top 50 of all calculated similarities. Through this threshold-based filtering, we discarded 21% of low-quality image-text pairs, retaining 79% to form a new pretraining dataset, Filtered-MALS.

Similarly, we also could filter the CUHK-PEDES training set in the fine-tuning phase to remove the noisy pair in the real-world

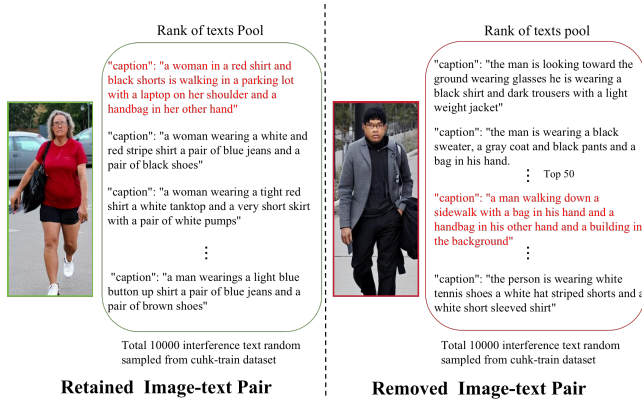


Figure 4: Visual explanation of data filtering. The part on the left of the image shows the high-quality image retained after our screening strategy and its corresponding red text description, while the person image on the right represents the low-quality image text pairs that are filtered out beyond the threshold, *i.e.*, top50. We deploy the real-world training set as distractors to filter low-relevance synthesized image-text pairs according to the similarity, since there are no overlaps.

training set. Employing the same calculation as in the first phase, we extract image features f_{I_C} and text features f_{T_C} for all pairs (I_C, T_C) . Each image calculates the cosine similarity with both the ground-truth text and a subset of 10,000 random and interference texts $f_{T_C'}$. Similarly, the similarity can be formulated as:

$$Sim_{self} = \cos(f_{I_C}, f_{T_C}), Sim_{other} = \cos(f_{I_C}, f_{T_C'}). \quad (2)$$

After computing and ranking these similarities for the entire training set, we set a relatively loose ranking threshold at 1800 considering most pairs are annotated by human. Through this selection process, 10% of low-quality image-text pairs are removed, leaving 90% to create a new fine-tuning dataset, Refined-CUHK, for model fine-tuning.

Discussion. The mechanism of filtering. The motivation is within the spectrum of generated datasets. (1) It is worth noting that not all contents bear relevance, with a portion comprising low-quality image-text pairs. Such instances of subpar alignment between textual descriptions and corresponding images can invariably exert a deleterious impact, compromising the model training. Predominantly, the segments of the dataset that contribute most significantly to the performance of the model are those encompassing high-quality data, often referred to as the ‘coreset’. (2) The extensive volume of data implicated in the pretraining phase incurs substantial computational costs, necessitating considerable resources in terms of computational power and temporal investment.

Therefore, there are two primary advantages of data filtering: (1) Initially, through the implementation of our filtering algorithm, we identify the core set of image-text pairs within the dataset that play a pivotal role in enhancing the quality of data fed into the model for learning. This strategic selection process facilitates the exposure of the model to higher-quality data, thereby augmenting its performance capabilities. (2) Subsequently, retaining the core set within the filtered dataset markedly reduces the overall volume of data,

which, in turn, diminishes the computational overhead involved in the training process. This efficiency gain leads to a reduction in both the requisite computational power and the temporal expenditure. Figure 4 shows an example of the data filtering process.

3.3 Weighted Low-Rank Adaptation

While the introduction of a pretrain-finetune paradigm to train models for person search tasks has achieved commendable results [68], the expansion in model and dataset sizes significantly increases the number of parameters to be trained, demanding substantial computational resources and sacrifices training efficiency. To address this issue, several parameter-efficient fine-tuning methods [19] have been proposed, aiming to fine-tune pretrained models using the minimum number of parameters. Among these, LoRA [20] has gained popularity due to its simplicity and efficacy. LoRA employs a low-rank decomposition for the pretrained weight matrix $W_0 \in \mathbb{R}^{m \times n}$, $W_0 + \Delta W = W_0 + BA$, where $B \in \mathbb{R}^{m \times r}$, $A \in \mathbb{R}^{r \times n}$, rank $r \ll \min(m, n)$. ΔW is adjusted by $\frac{\beta}{r}$. Inspired by the LoRA [20], which updates only a small part of the model weight to improve efficiency, DoRA [40] decomposes the weight into two parts: direction and amplitude. DoRA improves the adaptability and efficiency of the model, which can be formulated as $W_{DoRA} = m \frac{W_0 + BA}{\|W_0 + BA\|_2}$, where $m \in \mathbb{R}^{1 \times n}$ is the magnitude vector. $\|\cdot\|_2$ denotes the L2 norm of a matrix across each column.

However, these two methods still limit the parameter freedom. Therefore, we introduce the Weighted Low-Rank Adaptation (WoRA) model to address the capacity gap still present between LoRA [20] and fine-tuning (see Figure 2 right). Drawing from the DoRA [40] approach, which reparameterizes model weights into magnitude and direction components for fine-tuning, WoRA introduces new learnable parameters, α and β , to facilitate parameter learning. Given that pretrained weights already possess a vast repository of knowledge suitable for various downstream tasks, we configure these learnable parameters to ensure the model acquires sufficient capability in both magnitude and direction. This allows for the model to adapt to downstream tasks by updating parameters that exhibit significant magnitude or directional changes. The formal representation of our WoRA model is:

$$W_{WoRA} = m \frac{\beta * W_0 + \alpha * BA}{\|\beta * W_0 + \alpha * BA\|_2}. \quad (3)$$

In our model, parameters denoted with an overline represent trainable parameters. Our Weighted Low-Rank Adaptation (WoRA) achieves learning capabilities remarkably similar to those of fine-tuning. During inference, WoRA merges with pretrained weights, thereby not introducing any additional latency and enhancing the learnability and computational speed of the model. Furthermore, through the introduction of new learnable parameters, our WoRA indicates superior learning performance compared to both LoRA [20] and DoRA [40].

Discussion. Why WoRA better than LoRA and DoRA? As shown in Figure 5, both DoRA and LoRA are the specific cases of our proposed WoRA. In particular, DoRA can be derived by WoRA via setting $\alpha = 1$ and $\beta = 1$ as fixed constants. Further, if we set WoRA $\alpha = 1$, $\beta = 1$ and $m = 1$ as fixed constants, we will achieve the identical function as LoRA. **Time cost:** As WoRA adds

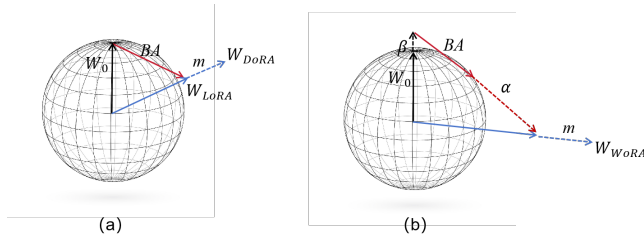


Figure 5: Intuitive explanation of WoRA. (a) We show weight changes for LoRA and DoRA (b) We show weight changes for WoRA, where BA represents weight direction rotation, and α , β , and m take charge of magnitude.

three trainable parameters compared with LoRA, it takes more time for the model to learn when calculating weights in the training stage. Although the time of WoRA is slightly slower than that of DoRA and LoRA, due to the addition of trainable parameters, better effects can be achieved by adjusting the weights. Please refer to the performance of the model in Table 5. A small amount of extra time (about 30 minutes) can promote the model fine-tuning capability by a clear margin. **Memory cost:** It is worth noting that our space complexity is the same as DoRA, while WoRA yields more direction and magnitude freedom, facilitating the fine-tuning process. WoRA only adds two constant learnable scalars of magnitude compared with DoRA during each weight update. Therefore, the increased consumption of space complexity in WoRA is negligible.

4 EXPERIMENT

4.1 Experimental Setup

Datasets. Our study encompasses processing and training on two datasets. For pretraining, we utilize the synthetic dataset, *i.e.*, MALS [68]. The MALS dataset contains 1,510,330 image-text pairs, with each pair annotated with appropriate attribute labels. For the fine-tuning phase, we employ CUHK-PEDES [34], RSTPReid [79] and ICFG-PEDES. CUHK-PEDES aggregates 40,206 images of 13,003 individuals from five existing person search datasets: CUHK03 [36], Market-1501 [74], SSM [65], VIPER [16], and CUHK01 [35], serving as subjects for language descriptions. Each image is annotated with descriptions from two sentences, amassing a total of 80,412 sentences. Our approach is evaluated on the public text-based person search dataset CUHK-PEDES. RSTPReid comprises 20,505 images of 4,101 people and is created by compiling MSMT17 [63]. ICFG-PEDES [12] is also created from MSMT17 and has 54,522 images of 4,102 individuals.

Evaluation metrics. We adopt the mean Average Precision (AP) and Recall@1,5,10 as our primary evaluation metrics. The Recall@K, whose value is 1 if the first matched image has appeared before the K-th image. Recall@K is sensitive to the position of the first matched image and suits the test set with only one true-matched image in the gallery. The average precision (AP) is the area under the PR(Precision-Recall) curve, considering all ground-truth images in the gallery. mAP is calculated and averaged for the average accuracy (AP) of each category.

Implementation Details. Our model with the proposed WoRA, undergoes pretraining across 32 epochs on 8 NVIDIA A800 GPUs

via Pytorch, adopting a batch size of 150. The optimization strategy employs the AdamW optimizer [43], integrating a weight decay factor of 0.01. Initiation of the learning rate is set at $1e^{-5}$, incorporating a warm-up phase over the initial 2600 steps, which then transitions into a linear decay schedule ranging from $1e^{-4}$ down to $1e^{-5}$. Image preprocessing includes resizing to 384×128 dimensions, coupled with augmentation strategies such as random horizontal flipping, RandAugment [10], and random erasing [78]. For the pretraining phase, the image encoder is initialized using Swin-B [42], enhanced by the application of the WoRA method. Both the text encoder and cross encoder commence with configurations derived from the initial and final 6 layers of Bert [11], respectively. Subsequent to the pretraining, the model is fine-tuned on designated downstream datasets over 30 epochs. Initial WoRA settings for the image encoder, rank = 8, $\alpha = 8$, and $\beta = 1$, are preserved, with the learning rate commencing at $1e^{-4}$. This phase includes a warm-up period spanning the first three epochs, succeeded by a methodical reduction of the learning rate according to a linear scheduler.

4.2 Comparison with Existing Methods

We deploy the Weighted Low-Rank Adaptation (WoRA) for text-based person search tasks. Performance comparisons are made using Recall@1,5,10 and mean Average Precision (mAP) metrics, alongside a comparison of parameter count (params in Millions, M) and computational efficiency (FLOPs) against the baseline model APTM. WoRA is evaluated on the CUHK-PEDES, RSTPReid and ICFG-PEDES datasets. In addition to image data augmentation mentioned during pretraining, Easy Data Augmentation (EDA) [62] was employed for text data augmentation, with the batch size set to 120. For each text query, its cosine similarity with all images was calculated, selecting the top 128 candidate images. Subsequently, the match probability between the text query and each selected image candidate was computed and ranked [68]. Through trainable adjustments to weight parameters, the WoRA method indicated robust performance across both datasets, significantly reducing computational parameters and time. Specifically, compared to APTM, which was trained on 1.51M data, our data filtering algorithm removed 21% of low-quality, noisy data, utilizing 1.19M data for computations. Our implementation of WoRA on the CUHK-PEDES dataset reduced trainable parameters to 127.37M, a 41% decrease from APTM, with FLOPs reduced to 23.21G, a 39% reduction. The overall training duration for pretraining and fine-tuning was cut by 19.82%, with our model achieving slight improvements in recall rates and mAP, as evidenced in Table 1. Moreover, the pretrained model adjusted through WoRA achieves competitive performance on the RSTPReid and ICFG-PEDES dataset, as shown in Table 2 and 3. To show the performance of our model more intuitively, we present three visual retrieval results on CUHK-PEDES in Figure 7. Our model adeptly captures fine-grained, word-level details, enabling it to accurately differentiate subtle variations in clothing colors among individuals. Furthermore, it exhibits robust retrieval capabilities, effectively identifying subjects even when parts of their details are obscured. This indicates the strong performance of our model in handling nuanced visual variations and partial occlusions within complex scenes.

Method	#Parameter	R@1	R@5	R@10	mAP
CNN-RNN [50]	-	8.07	-	32.47	-
GNA-RNN [34]	-	19.05	-	53.64	-
PWM-ATH [7]	-	27.14	49.45	61.02	-
GLA [6]	-	43.58	66.93	76.2	-
Dual Path [76]	-	44.40	66.26	75.07	-
CMPM+CMPC [72]	-	49.37	-	79.21	-
MIA [45]	-	53.10	75.00	82.90	-
A-GANet [39]	-	53.14	74.03	81.95	-
ViTAA [58]	-	55.97	75.84	83.52	51.60
IMG-Net [61]	-	56.48	76.89	85.01	-
CMAAM [1]	-	56.68	77.18	84.86	-
HGAN [73]	-	59.00	79.49	86.62	-
NAFS [15]	-	59.94	79.86	86.70	54.07
DSSL [79]	-	59.98	80.41	87.56	-
MGEL [56]	-	60.27	80.01	86.74	-
SSAN [12]	-	61.37	80.15	86.73	-
NAFS [15]	-	61.50	81.19	87.51	-
TBPS [17]	-	61.65	80.98	86.78	-
TIPCB [8]	-	63.63	82.82	89.01	-
LBUL [60]	-	64.04	82.66	87.22	-
CAIBC [59]	-	64.43	82.87	88.37	-
AXM-Net [13]	-	64.44	80.52	86.77	58.73
LGUR [53]	-	65.25	83.12	89.00	-
CFine [67]	-	69.57	85.93	91.15	-
VGSG [18]	-	71.38	86.75	91.86	67.91
TBPS-CLIP [4]	149M	73.54	88.19	92.35	65.38
IRRA [23]	194M	73.38	89.93	93.71	66.13
RaSa [3]	210M	76.51	90.29	94.25	69.38
APTМ [68]	214M	76.53	90.04	94.15	66.91
Baseline*	214M	75.42	88.86	92.77	66.61
Ours	127M	76.38	89.72	93.49	67.22

Table 1: Performance Comparison on CUHK-PEDES. Here we show the performance of the previous methods on the recall@1,5,10, mAP in % and the parameter number. Baseline*: We re-implement APTM [68].

4.3 Ablation Study and Further Discussion

The impact of data filtering. Here, “baseline” refers to the APTM method as implemented in our experimental setup, and “top50” denotes our data filtering approach with a threshold set to top50 for selecting the pre-training dataset MALS. From Table 4, it is evident that training the pre-trained models with our filtered dataset results in improvements of 6.26% in Recall@1, demonstrating the efficacy of our dataset filtering for pre-training. Similarly, we find the filtering on the downstream dataset also facilitates the learning, since the filtering algorithm generally removes the noise. In Table 5, the notation “ft90%” signifies the use of our dataset filtering method to refine the finetune dataset CUHK-PEDES, ultimately retaining 90% of its data for training. The model trained after applying “ft90%” exhibits a 0.25% increase in Recall@1, substantiating the effectiveness of dataset filtering on the comprehensive model.

Method	#Parameter	R@1	R@5	R@10	mAP
DSSL [79]	-	32.43	55.08	63.19	-
LBUL [60]	-	45.55	68.20	77.85	-
IVT [54]	-	46.70	70.00	78.80	-
CAIBC [59]	-	47.35	69.55	79.00	-
CFine [67]	-	50.55	72.50	81.60	-
TBPS-CLIP [4]	149M	61.95	83.55	88.75	48.26
IRRA [23]	194M	60.20	81.30	88.20	47.17
RaSa [3]	210M	66.90	86.50	91.35	52.31
APTМ [68]	214M	67.50	85.70	91.45	52.56
Baseline*	214M	66.40	85.55	91.10	52.21
Ours	127M	66.85	86.45	91.10	52.49

Table 2: Performance Comparison on RSTPReid. Here we show the performance of the previous methods on the recall@1,5,10 and mAP in % and the parameter number. Baseline*: We re-implement APTM [68].

Method	#Parameter	R@1	R@5	R@10	mAP
Dual Path [76]	-	38.99	59.44	68.41	-
CMPM+CMPC [72]	-	43.51	65.44	74.26	-
MIA [45]	-	46.49	67.14	75.18	-
SCAN [27]	-	50.05	69.65	77.21	-
ViTAA [58]	-	50.98	68.79	75.78	-
SSAN [12]	-	54.23	72.63	79.53	-
IVT [54]	-	56.04	73.60	80.22	-
LGUR [53]	-	59.02	75.32	81.56	-
CFine [67]	-	60.83	76.55	82.42	-
TBPS-CLIP [4]	149M	65.05	80.34	85.47	39.83
IRRA [23]	194M	63.46	80.25	85.82	38.06
RaSa [3]	210M	65.28	80.04	85.12	41.29
APTМ [68]	214M	68.51	82.99	87.56	41.22
Baseline*	214M	67.81	82.70	87.32	41.22
Ours	127M	68.35	83.10	87.53	42.60

Table 3: Performance Comparison on ICFG-PEDES. Here we show the performance of the previous methods on the recall@1,5,10 and mAP in % and the parameter number. Baseline*: We re-implement APTM [68].

The impact of WoRA. We further investigate the impact of Low-Rank Adaptation on pre-training, where “WoRA” in Table 4 and 5 signifies our Weighted Low-Rank Adaptation approach. Implementing WoRA in the pre-trained models led to a +6.72% boost in Recall@1 and a +6.71% enhancement in mAP, concurrently reducing the time by 22.22%, thereby validating the efficiency of our dataset filtering and WoRA in model pre-training. Moreover, we assess the impact of Weighted Low-Rank Adaptation (WoRA) on the complete model. Initially, comparing the impacts of using LoRA [20] and DoRA [40] models of Low-Rank Adaptation on our fully trained model revealed improvements in model speed but not in performance. Subsequently, applying WoRA to models trained on the top50 pre-training selection and the ft90% finetuned dataset, we achieved a Recall@1 of 76.38%, surpassing the baseline by 0.96%, and an mAP of 67.22%, exceeding the baseline by 0.61%, thereby

Method	# Data (M)	# Trainable Params (M)	Flops (G)	CUHK-PEDES		RSTPReid		ICFG-PEDES		Time (hours)
				R@1	mAP	R@1	mAP	R@1	mAP	
Pretraining Stage										
Baseline* (APTM [68])	1.51M	213.99 M	38.02 G	3.99	3.62	4.40	3.95	0.77	0.59	18h
Ours (top50)	1.19M	213.99 M	38.00 G	10.25	10.24	12.65	9.37	8.07	2.35	14h
Ours (top50+WoRA)	1.19M	127.37 M	23.21 G	10.71	10.33	13.00	9.59	10.80	3.10	14h
Finetune Stage										
Baseline* (APTM [68])	0.068M	213.99 M	44.93 G	75.42	66.61	66.32	52.30	67.66	41.98	4.2h
Ours (top50)	0.061M	213.99 M	44.93 G	75.67	66.27	66.40	52.21	67.80	42.38	3.8h
Ours (top50+WoRA)	0.061M	127.37 M	30.13 G	76.38	67.22	66.85	52.49	68.35	42.60	3.8h

Table 4: Compared with APTM method at recall@1 and mAP results on CUHK-PEDES, RSTPReid and ICFG-PEDES. Meanwhile, we also compare the data volume, params (M) and Flops (G) of the model. Ablation study about our methods on pretrain. The top50 denotes the results trained by using a pre-trained dataset filtered using a data filtering method. The top50+WoRA is our ultimate two-stage approach, and by adding WoRA to fine-tune the model, we can improve the performance of the pre-trained model while saving 19.82% training time.

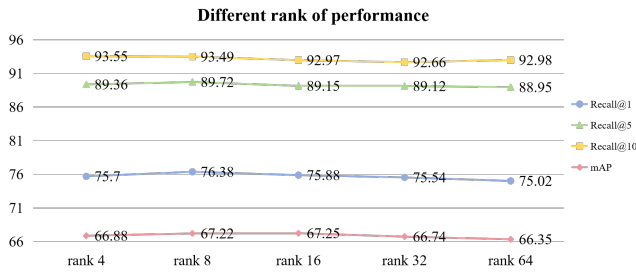


Figure 6: The impact of different WoRA ranks on performance. We observe that the result is not sensitive to the rank. Generally, rank=8 is the best hyper-parameter in terms of performance on Recall@1,5,10.

Method	top50	ft 90%	R@1	mAP
Baseline*			75.42	66.61
Baseline*	✓		75.83	66.70
Baseline*	✓	✓	75.67	66.27
LoRA	✓		74.40	64.95
LoRA	✓	✓	74.29 (-1.38)	65.59 (-0.68)
DoRA	✓		75.49	66.92
DoRA	✓	✓	75.73 (+0.06)	66.75 (+0.48)
WoRA (Ours)	✓		75.67	67.09
WoRA (Ours)	✓	✓	76.38 (+0.71)	67.22 (+0.95)

Table 5: Comparison of our WoRA with baseline, LoRA and DoRA in the different situations. Finally, the experiment shows that our methods achieve the best recall@1 and mAP in %. ft 90% denotes the use of our dataset filtering method to refine the finetune dataset CUHK-PEDES, ultimately retaining 90% of its data for training, while top50 is using a data filtering approach with a threshold set to top50 for selecting the pre-training dataset MALS.

Text Query

The man is facing away and walking in strappy sandals he wears a cross body bag a watch and tan shorts with a gray blue short sleeved shirt he has short dark hair

A woman wearing a light blue shirt a pair of black shorts and a pair of black and brown shoes

She has her long black hair in a pony tail she is also wearing a colorful shirt and light colored pants

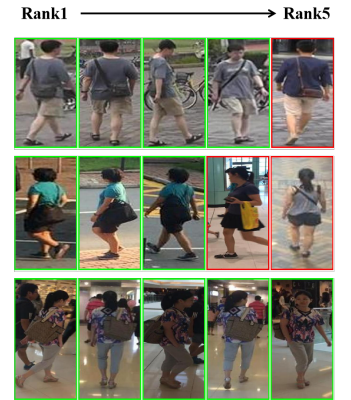


Figure 7: Qualitative person search results using text query of our methods, placing in descending order from left to right based on matching probability. The images in green boxes are the correct matches, and the images in red boxes are the wrong matches. The green texts show that our results successfully match.

establishing state-of-the-art (SOTA) mAP performance. The computation time for the complete model is reduced from 23h to 18h, marking a 19.82% acceleration. In Figure 6, we compare the effects of different rank values on the performance of WoRA. The experiment shows that the model has the best performance on Recall@1,5,10 when rank is equal to 8. We can observe that model performance may not be as sensitive in different ranks. Performance can be improved basically with the WoRA model. The results we present in this paper are obtained using rank=8, which has achieved the best performance on Recall@1,5,10. As shown in Table 5, we could observe two points (1) WoRA is better than both LoRA and DoRA, whether the performance of Recall@1 or mAP. (2) Furthermore, if we both use the top50 and ft90% filtering strategy, WoRA is also the best performing, which surpasses the baseline by 0.71% Recall@1 and 0.95% mAP under the same conditions.

5 CONCLUSION

In this work, we introduce a new Filtering-WoRA paradigm, which contains a filtering algorithm to identify this crucial data subset and WoRA layers (Weighted Low-Rank Adaptation) for light fine-tuning. Filtering strategy for image-text pairs within language-based person search datasets, designed to isolate a core set from large-scale, noise-containing datasets of generated image-text pairs. WoRA (Weighted Low-Rank Adaptation) learning strategy to efficiently update the portion of model parameters. Extensive experiments indicate that our approach is 19.82% faster than existing language-based person search methods while maintaining comparable accuracy with state-of-the-art (SOTA) language-based person search models. On three public benchmarks, CUHK-PEDES, RSTPReeid, and ICFG-PEDES, our method achieves competitive recall rates and mean Average Precision (mAP).

REFERENCES

- [1] Surbhi Aggarwal, R. Venkatesh Babu, and Anirban Chakraborty. 2020. Text-based Person Search via Attribute-aided Matching. In *2020 IEEE Winter Conference on Applications of Computer Vision (WACV)*. 2606–2614. <https://doi.org/10.1109/WACV45572.2020.9093640>
- [2] Peter Anderson, Xiaodong He, Chris Buehler, Damien Teney, Mark Johnson, Stephen Gould, and Lei Zhang. 2018. Bottom-Up and Top-Down Attention for Image Captioning and Visual Question Answering. In *2018 IEEE/CVF Conference on Computer Vision and Pattern Recognition (CVPR)*. <https://doi.org/10.1109/cvpr.2018.00636>
- [3] Yang Bai, Min Cao, Daming Gao, Ziqiang Cao, Chen Chen, Zhenfeng Fan, Liqiang Nie, and Min Zhang. 2023. RaSa: Relation and Sensitivity Aware Representation Learning for Text-based Person Search. In *Proceedings of the Thirty-Second International Joint Conference on Artificial Intelligence (IJCAI-2023)*. International Joint Conferences on Artificial Intelligence Organization. <https://doi.org/10.24963/ijcai.2023/62>
- [4] Min Cao, Yang Bai, Ziyin Zeng, Mang Ye, and Min Zhang. 2023. An Empirical Study of CLIP for Text-based Person Search. *arXiv preprint arXiv:2308.10045* (2023).
- [5] Nicolas Carion, Francisco Massa, Gabriel Synnaeve, Nicolas Usunier, Alexander Kirillov, and Sergey Zagoruyko. 2020. *End-to-End Object Detection with Transformers*. 213–229. https://doi.org/10.1007/978-3-030-58452-8_13
- [6] Dapeng Chen, Hongsheng Li, Xihui Liu, Yantao Shen, Jing Shao, Zejian Yuan, and Xiaogang Wang. 2018. Improving Deep Visual Representation for Person Re-identification by Global and Local Image-language Association. In *Computer Vision – ECCV 2018: 15th European Conference, Munich, Germany, September 8–14, 2018, Proceedings, Part XVI* (Munich, Germany). Springer-Verlag, Berlin, Heidelberg, 56–73. https://doi.org/10.1007/978-3-030-01270-0_4
- [7] Tianlang Chen, Chenliang Xu, and Jiebo Luo. 2018. Improving Text-Based Person Search by Spatial Matching and Adaptive Threshold. In *2018 IEEE Winter Conference on Applications of Computer Vision (WACV)*. 1879–1887. <https://doi.org/10.1109/WACV.2018.00208>
- [8] Yuhao Chen, Guoqing Zhang, Yujiang Lu, Zhenxing Wang, and Yuhui Zheng. 2022. TIPCB: A simple but effective part-based convolutional baseline for text-based person search. *Neurocomputing* (Jul 2022), 171–181. <https://doi.org/10.1016/j.neucom.2022.04.081>
- [9] Yen-Chun Chen, Linjie Li, Licheng Yu, Ahmed El Kholy, Faisal Ahmed, Zhe Gan, Yu Cheng, and Jingjing Liu. 2020. *UNITER: UNiversal Image-Text Representation Learning*. 104–120. https://doi.org/10.1007/978-3-030-58577-8_7
- [10] Ekin D. Cubuk, Barret Zoph, Jonathon Shlens, and Quoc V. Le. 2020. Randaugment: Practical automated data augmentation with a reduced search space. In *2020 IEEE/CVF Conference on Computer Vision and Pattern Recognition Workshops (CVPRW)*. <https://doi.org/10.1109/cvprw50498.2020.00359>
- [11] Jacob Devlin, Ming-Wei Chang, Kenton Lee, and Kristina Toutanova. 2019. BERT: Pre-training of Deep Bidirectional Transformers for Language Understanding. *arXiv:1810.04805* [cs.CL]
- [12] Zefeng Ding, Changxing Ding, Zhiyin Shao, and Dacheng Tao. 2021. Semantically Self-Aligned Network for Text-to-Image Part-aware Person Re-identification. *arXiv: Computer Vision and Pattern Recognition, arXiv: Computer Vision and Pattern Recognition* (Jul 2021).
- [13] Ammarah Farooq, Muhammad Awais, Josef Kittler, and Syed Safwan Khalid. 2022. AXM-Net: Implicit Cross-Modal Feature Alignment for Person Re-identification. *Proceedings of the AAAI Conference on Artificial Intelligence* 36, 4 (Jun. 2022), 4477–4485. <https://doi.org/10.1609/aaai.v36i4.20370>
- [14] Zhe Gan, Yen-Chun Chen, Pingqing Fu, Chen Zhu, Yu Cheng, and Jingjing Liu. 2020. Large-Scale Adversarial Training for Vision-and-Language Representation Learning. *Neural Information Processing Systems, Neural Information Processing Systems* (Jun 2020).
- [15] Chenyang Gao, Guanyu Cai, Xinyang Jiang, Feng Zheng, Jun Zhang, Yifei Gong, Pai Peng, Xiaowei Guo, and Xing Sun. 2021. Contextual Non-Local Alignment over Full-Scale Representation for Text-Based Person Search. *arXiv:2101.03036* [cs.CV]
- [16] Douglas A. Gray, Shane Brennan, and Hai Tao. 2007. Evaluating Appearance Models for Recognition, Reacquisition, and Tracking. (Jan 2007).
- [17] Xiao Han, Sen He, Li Zhang, and Tao Xiang. 2021. Text-Based Person Search with Limited Data. *arXiv:2110.10807* [cs.CV]
- [18] Shuting He, Hao Luo, Wei Jiang, Xudong Jiang, and Henghui Ding. 2024. VGSG: Vision-Guided Semantic-Group Network for Text-Based Person Search. *IEEE Transactions on Image Processing* 33 (2024), 163–176. <https://doi.org/10.1109/TIP.2023.3337653>
- [19] Neil Houlsby, Andrei Giurgiu, Stanislaw Jastrzebski, Bruna Morrone, Quentin de Laroussilhe, Andrea Gesmundo, Mona Attariyan, and Sylvain Gelly. 2019. Parameter-Efficient Transfer Learning for NLP. *arXiv:1902.00751* [cs.LG]
- [20] Edward J. Hu, Yelong Shen, Phillip Wallis, Zeyuan Allen-Zhu, Yuanzhi Li, Shean Wang, Lu Wang, and Weizhu Chen. 2021. LoRA: Low-Rank Adaptation of Large Language Models. *arXiv:2106.09685* [cs.CL]
- [21] Zhicheng Huang, Zhaoyang Zeng, Yupan Huang, Bei Liu, Dongmei Fu, and Jianlong Fu. 2021. Seeing Out of the box: End-to-End Pre-training for Vision-Language Representation Learning. 12971–12980. <https://doi.org/10.1109/CVPR46437.2021.01278>
- [22] Zhicheng Huang, Zhaoyang Zeng, Bei Liu, Dongmei Fu, and Jianlong Fu. 2020. Pixel-BERT: Aligning Image Pixels with Text by Deep Multi-Modal Transformers. *arXiv: Computer Vision and Pattern Recognition, arXiv: Computer Vision and Pattern Recognition* (Apr 2020).
- [23] Ding Jiang and Mang Ye. 2023. Cross-Modal Implicit Relation Reasoning and Aligning for Text-to-Image Person Retrieval. In *IEEE International Conference on Computer Vision and Pattern Recognition (CVPR)*.
- [24] Huaizu Jiang, Ishan Misra, Marcus Rohrbach, Erik Learned-Miller, and Xinlei Chen. 2020. In Defense of Grid Features for Visual Question Answering. In *2020 IEEE/CVF Conference on Computer Vision and Pattern Recognition (CVPR)*. <https://doi.org/10.1109/cvpr42600.2020.01028>
- [25] Won-Jae Kim, Bokyoung Son, and Ildoo Kim. 2021. ViLT: Vision-and-Language Transformer Without Convolution or Region Supervision. *Cornell University - arXiv, Cornell University - arXiv* (Feb 2021).
- [26] Ranjay Krishna, Yuke Zhu, Oliver Groth, Justin Johnson, Kenji Hata, Joshua Kravitz, Stephanie Chen, Yannis Kalantidis, Li-Jia Li, David A. Shamma, Michael S. Bernstein, and Li Fei-Fei. 2017. Visual Genome: Connecting Language and Vision Using Crowdsourced Dense Image Annotations. *International Journal of Computer Vision* (May 2017), 32–73. <https://doi.org/10.1007/s11263-016-0981-7>
- [27] Kuang-Huei Lee, Xi Chen, Gang Hua, Houdong Hu, and Xiaodong He. 2018. Stacked Cross Attention for Image-Text Matching. *arXiv:1803.08024* [cs.CV]
- [28] Gen Li, Nan Duan, Yuejian Fang, Ming Gong, and Daxin Jiang. 2020. Unicoder-VL: A Universal Encoder for Vision and Language by Cross-modal Pre-training. *Proceedings of the AAAI Conference on Artificial Intelligence* (Jun 2020), 11336–11344. <https://doi.org/10.1609/aaai.v34i07.6795>
- [29] Junnan Li, Dongxu Li, Silvio Savarese, and Steven Hoi. 2023. BLIP-2: bootstrapping language-image pre-training with frozen image encoders and large language models. In *Proceedings of the 40th International Conference on Machine Learning* (, Honolulu, Hawaii, USA.) (ICML '23). JMLR.org, Article 814, 13 pages.
- [30] Junnan Li, Dongxu Li, Caiming Xiong, and Steven Hoi. 2022. BLIP: Bootstrapping Language-Image Pre-training for Unified Vision-Language Understanding and Generation. In *Proceedings of the 39th International Conference on Machine Learning (Proceedings of Machine Learning Research, Vol. 162)*. Kamalika Chaudhuri, Stefanie Jegelka, Le Song, Csaba Szepesvari, Gang Niu, and Sivan Sabato (Eds.). PMLR, 12888–12900. <https://proceedings.mlr.press/v162/li22n.html>
- [31] Junnan Li, Ramprasaath R. Selvaraju, Akhilesh Gotmare, Shafiq Joty, Caiming Xiong, and Steven C.H. Hoi. 2021. Align before Fuse: Vision and Language Representation Learning with Momentum Distillation. *Cornell University - arXiv, Cornell University - arXiv* (Jul 2021).
- [32] Liunian Harold Li, Mark Yatskar, Dong Yin, Cho-Jui Hsieh, and Kai-Wei Chang. 2019. VisualBERT: A Simple and Performant Baseline for Vision and Language. *Cornell University - arXiv, Cornell University - arXiv* (Aug 2019).
- [33] Shuang Li, Tong Xiao, Hongsheng Li, Wei Yang, and Xiaogang Wang. 2017. Identity-Aware Textual-Visual Matching with Latent Co-attention. *Cornell University - arXiv, Cornell University - arXiv* (Aug 2017).
- [34] Shuang Li, Tong Xiao, Hongsheng Li, Bolei Zhou, Dayu Yue, and Xiaogang Wang. 2017. Person Search with Natural Language Description. In *2017 IEEE Conference on Computer Vision and Pattern Recognition (CVPR)*. <https://doi.org/10.1109/cvpr.2017.551>
- [35] Wei Li, Rui Zhao, and Xiaogang Wang. 2013. *Human Reidentification with Transferred Metric Learning*. 31–44. https://doi.org/10.1007/978-3-642-37331-2_3

- [36] Wei Li, Rui Zhao, Tong Xiao, and Xiaogang Wang. 2014. DeepReID: Deep Filter Pairing Neural Network for Person Re-identification. In *2014 IEEE Conference on Computer Vision and Pattern Recognition*. <https://doi.org/10.1109/cvpr.2014.27>
- [37] Xiujun Li, Xi Yin, Chunyuan Li, Pengchuan Zhang, Xiaowei Hu, Lei Zhang, Lijuan Wang, Houdong Hu, Li Dong, Furu Wei, Yejin Choi, and Jianfeng Gao. 2020. *Oscar: Object-Semantics Aligned Pre-training for Vision-Language Tasks*. 121–137. https://doi.org/10.1007/978-3-030-58577-8_8
- [38] Tsung-Yi Lin, Michael Maire, Serge Belongie, James Hays, Pietro Perona, Deva Ramanan, Piotr Dollár, and C. Lawrence Zitnick. 2014. *Microsoft COCO: Common Objects in Context*. 740–755. https://doi.org/10.1007/978-3-319-10602-1_48
- [39] Jiawei Liu, Zheng-Jun Zha, Richang Hong, Meng Wang, and Yongdong Zhang. 2019. Deep Adversarial Graph Attention Convolution Network for Text-Based Person Search. In *Proceedings of the 27th ACM International Conference on Multimedia (Nice, France) (MM '19)*. Association for Computing Machinery, New York, NY, USA, 665–673. <https://doi.org/10.1145/3343031.3350991>
- [40] Shih-Yang Liu, Chien-Yi Wang, Hongxu Yin, Pavlo Molchanov, Yu-Chiang Frank Wang, Kwang-Ting Cheng, and Min-Hung Chen. 2024. DoRA: Weight-Decomposed Low-Rank Adaptation. arXiv:2402.09353 [cs.CL]
- [41] Yongfei Liu, Chenfei Wu, Shao-Yen Tseng, Vasudev Lal, Xuming He, and Nan Duan. 2022. KD-VLP: Improving End-to-End Vision-and-Language Pretraining with Object Knowledge Distillation. In *Findings of the Association for Computational Linguistics: NAACL 2022*. <https://doi.org/10.18653/v1/2022.findings-naacl.119>
- [42] Ze Liu, Yutong Lin, Yue Cao, Han Hu, Yixuan Wei, Zheng Zhang, Stephen Lin, and Baining Guo. 2021. Swin Transformer: Hierarchical Vision Transformer using Shifted Windows. In *2021 IEEE/CVF International Conference on Computer Vision (ICCV)*. <https://doi.org/10.1109/iccv48922.2021.00986>
- [43] Ilya Loshchilov and Frank Hutter. 2017. Decoupled Weight Decay Regularization. *Learning.Learning* (Nov 2017).
- [44] Jing Lu, Dhruv Batra, Devi Parikh, and Stefan Lee. 2019. ViLBERT: Pretraining Task-Agnostic Visiolinguistic Representations for Vision-and-Language Tasks. *Neural Information Processing Systems, Neural Information Processing Systems* (Aug 2019).
- [45] Kai Niu, Yan Huang, Wanli Ouyang, and Liang Wang. 2019. Improving Description-based Person Re-identification by Multi-granularity Image-text Alignments. arXiv:1906.09610 [cs.CV]
- [46] Zhiliang Peng, Dong Li, Hangbo Bao, Qixiang Ye, and Furu Wei. [n. d.]. BEIT V2: Masked Image Modeling with Vector-Quantized Visual Tokenizers. [n. d.].
- [47] Dustin Podell, Zion English, Kyle Lacey, Andreas Blattmann, Tim Dockhorn, Jonas Müller, Joe Penna, and Robin Rombach. 2023. SDXL: Improving Latent Diffusion Models for High-Resolution Image Synthesis. arXiv:2307.01952 [cs.CV]
- [48] Filip Radenovic, Abhimanyu Dubey, Abhishek Kadian, Todor Mihaylov, Simon Vandenhende, Yash Patel, Yi Wen, Vignesh Ramanathan, and Dhruv Mahajan. 2023. Filtering, Distillation, and Hard Negatives for Vision-Language Pre-Training. arXiv:2301.02280 [cs.CV]
- [49] Alec Radford, JongWook Kim, Chris Hallacy, A. Ramesh, Gabriel Goh, Sandhini Agarwal, Girish Sastry, Askell Amanda, Pamela Mishkin, Jack Clark, Gretchen Krueger, and Ilya Sutskever. 2021. Learning Transferable Visual Models From Natural Language Supervision. *Cornell University - arXiv, Cornell University - arXiv* (Feb 2021).
- [50] Scott Reed, Zeynep Akata, Bernt Schiele, and Honglak Lee. 2016. Learning Deep Representations of Fine-grained Visual Descriptions. arXiv:1605.05395 [cs.CV]
- [51] Shaoqing Ren, Kaiming He, Ross Girshick, and Jian Sun. 2017. Faster R-CNN: Towards Real-Time Object Detection with Region Proposal Networks. *IEEE Transactions on Pattern Analysis and Machine Intelligence* (Jun 2017), 1137–1149. <https://doi.org/10.1109/tpami.2016.2577031>
- [52] Robin Rombach, Andreas Blattmann, Dominik Lorenz, Patrick Esser, and Björn Ommer. 2022. High-Resolution Image Synthesis with Latent Diffusion Models. In *2022 IEEE/CVF Conference on Computer Vision and Pattern Recognition (CVPR)*. 10674–10685. <https://doi.org/10.1109/CVPR52688.2022.01042>
- [53] Zhiyin Shao, Xinyu Zhang, Meng Fang, Zhifeng Lin, Jian Wang, and Changxing Ding. 2022. Learning Granularity-Unified Representations for Text-to-Image Person Re-identification. (Jul 2022).
- [54] Xiujun Shu, Wei Wen, Haoqian Wu, Keyu Chen, Yiran Song, Ruizhi Qiao, Bo Ren, and Xiao Wang. 2022. See Finer, See More: Implicit Modality Alignment for Text-based Person Retrieval. (Aug 2022).
- [55] Hao Tan and Mohit Bansal. 2019. LXMERT: Learning Cross-Modality Encoder Representations from Transformers. In *Proceedings of the 2019 Conference on Empirical Methods in Natural Language Processing and the 9th International Joint Conference on Natural Language Processing (EMNLP-IJCNLP)*. <https://doi.org/10.18653/v1/d19-1514>
- [56] Chengji Wang, Zhiming Luo, Yaojin Lin, and Shaozi Li. 2021. Text-based Person Search via Multi-Granularity Embedding Learning. In *International Joint Conference on Artificial Intelligence*. <https://api.semanticscholar.org/CorpusID:237100188>
- [57] Peng Wang, An Yang, Rui Men, Junyang Lin, Shuai Bai, Zhikang Li, Jianxin Ma, Chang Zhou, Jingren Zhou, and Hongxia Yang. 2022. OFA: Unifying Architectures, Tasks, and Modalities Through a Simple Sequence-to-Sequence Learning Framework. arXiv:2202.03052 [cs.CV]
- [58] Zhe Wang, Zhiyuan Fang, Jun Wang, and Yezhou Yang. 2020. ViTAA: Visual-Textual Attributes Alignment in Person Search by Natural Language. arXiv:2005.07327 [cs.CV]
- [59] Zijie Wang, Aichun Zhu, Jingyi Xue, Xili Wan, Chao Liu, Tian Wang, and Yifeng Li. 2022. CAIBC: Capturing All-round Information Beyond Color for Text-based Person Retrieval. In *Proceedings of the 30th ACM International Conference on Multimedia*. <https://doi.org/10.1145/3503161.3548057>
- [60] Zijie Wang, Aichun Zhu, Jingyi Xue, Xili Wan, Chao Liu, Tian Wang, and Yifeng Li. 2022. Look Before You Leap: Improving Text-based Person Retrieval by Learning A Consistent Cross-modal Common Manifold. In *Proceedings of the 30th ACM International Conference on Multimedia*. <https://doi.org/10.1145/3503161.3548166>
- [61] Zijie Wang, Aichun Zhu, Zhe Zheng, Jing Jin, Zhouxin Xue, and Gang Hua. 2020. IMG-Net: inner-cross-modal attentional multigranular network for description-based person re-identification. *Journal of Electronic Imaging* 29 (2020), 043028–043028. <https://api.semanticscholar.org/CorpusID:221380389>
- [62] Jason Wei and Kai Zou. 2019. EDA: Easy Data Augmentation Techniques for Boosting Performance on Text Classification Tasks. In *Proceedings of the 2019 Conference on Empirical Methods in Natural Language Processing and the 9th International Joint Conference on Natural Language Processing (EMNLP-IJCNLP)*. <https://doi.org/10.18653/v1/d19-1670>
- [63] Longhui Wei, Shiliang Zhang, Wen Gao, and Qi Tian. 2018. Person Transfer GAN to Bridge Domain Gap for Person Re-Identification. In *2018 IEEE/CVF Conference on Computer Vision and Pattern Recognition*. <https://doi.org/10.1109/cvpr.2018.00016>
- [64] Kindi Wu, Byron Zhang, Zhiwei Deng, and Olga Russakovsky. 2024. Vision-Language Dataset Distillation. arXiv:2308.07545 [cs.CV]
- [65] Tong Xiao, Shuang Li, Bochao Wang, Lin Li, and Xiaogang Wang. 2016. End-to-End Deep Learning for Person Search. arXiv: *Computer Vision and Pattern Recognition, arXiv: Computer Vision and Pattern Recognition* (Apr 2016).
- [66] Haiyang Xu, Ming Yan, Chenliang Li, Bin Bi, Songfang Huang, Wenming Xiao, and Fei Huang. 2021. E2E-VLP: End-to-End Vision-Language Pre-training Enhanced by Visual Learning. In *Proceedings of the 59th Annual Meeting of the Association for Computational Linguistics and the 11th International Joint Conference on Natural Language Processing (Volume 1: Long Papers)*. <https://doi.org/10.18653/v1/2021.acl-long.42>
- [67] Shuanglin Yan, Neng Dong, Liyan Zhang, and Jinhui Tang. 2023. CLIP-Driven Fine-Grained Text-Image Person Re-Identification. *IEEE Transactions on Image Processing* 32 (2023), 6032–6046. <https://doi.org/10.1109/TIP.2023.3327924>
- [68] Shuyi Yang, Yinan Zhou, Yaxiong Wang, Yujiao Wu, Li Zhu, and Zhedong Zheng. 2023. Towards Unified Text-based Person Retrieval: A Large-scale Multi-Attribute and Language Search Benchmark. In *Proceedings of the 2023 ACM on Multimedia Conference*.
- [69] Yan Zeng, Xinsong Zhang, and Hang Li. 2022. Multi-Grained Vision Language Pre-Training: Aligning Texts with Visual Concepts. arXiv:2111.08276 [cs.CL]
- [70] Yan Zeng, Xinsong Zhang, Hang Li, Jiawei Wang, Jipeng Zhang, and Wangchunshu Zhou. 2022. X2-VLM: All-In-One Pre-trained Model For Vision-Language Tasks. arXiv:2211.12402 (2022).
- [71] Pengchuan Zhang, Xiujun Li, Xiaowei Hu, Jianwei Yang, Lei Zhang, Lijuan Wang, Yejin Choi, and Jianfeng Gao. 2021. VinVL: Revisiting Visual Representations in Vision-Language Models. In *2021 IEEE/CVF Conference on Computer Vision and Pattern Recognition (CVPR)*. <https://doi.org/10.1109/cvpr46437.2021.00553>
- [72] Ying Zhang and Huchuan Lu. 2018. Deep Cross-Modal Projection Learning for Image-Text Matching. In *Computer Vision – ECCV 2018*, Vittorio Ferrari, Martial Hebert, Cristian Sminchisescu, and Yair Weiss (Eds.). Springer International Publishing, Cham, 707–723.
- [73] Kecheng Zheng, Wu Liu, Jiawei Liu, Zheng-Jun Zha, and Tao Mei. 2020. Hierarchical Gumbel Attention Network for Text-based Person Search. In *Proceedings of the 28th ACM International Conference on Multimedia (Seattle, WA, USA) (MM '20)*. Association for Computing Machinery, New York, NY, USA, 3441–3449. <https://doi.org/10.1145/3394171.3413864>
- [74] Liang Zheng, Liyue Shen, Lei Tian, Shengjin Wang, Jiahao Bu, and Qi Tian. 2015. Person Re-identification Meets Image Search. arXiv: *Computer Vision and Pattern Recognition, arXiv: Computer Vision and Pattern Recognition* (Feb 2015).
- [75] Zhedong Zheng, Xiaodong Yang, Zhiding Yu, Liang Zheng, Yi Yang, and Jan Kautz. 2019. Joint discriminative and generative learning for person re-identification. In *proceedings of the IEEE/CVF conference on computer vision and pattern recognition*. 2138–2147.
- [76] Zhedong Zheng, Liang Zheng, Michael Garrett, Yi Yang, Mingliang Xu, and Yi-Dong Shen. 2020. Dual-Path Convolutional Image-Text Embedding with Instance Loss. *ACM Transactions on Multimedia Computing, Communications, and Applications* (May 2020), 1–23. <https://doi.org/10.1145/3383184>
- [77] Zhedong Zheng, Liang Zheng, and Yi Yang. 2017. Unlabeled samples generated by gan improve the person re-identification baseline in vitro. In *Proceedings of the IEEE international conference on computer vision*. 3754–3762.
- [78] Zhun Zhong, Liang Zheng, Guoliang Kang, Shaozi Li, and Yi Yang. 2020. Random Erasing Data Augmentation. *Proceedings of the AAAI Conference on Artificial Intelligence* (Jun 2020), 13001–13008. <https://doi.org/10.1609/aaai.v34i07.7000>

- [79] Aichun Zhu, Zijie Wang, Yifeng Li, Xili Wan, Jing Jin, Tian Wang, Fangqiang Hu, and Gang Hua. 2021. DSSL: Deep Surroundings-person Separation Learning for Text-based Person Retrieval. In *Proceedings of the 29th ACM International Conference on Multimedia (Virtual Event, China) (MM '21)*. Association for Computing Machinery, New York, NY, USA, 209–217. <https://doi.org/10.1145/3474085>.
- [80] Xizhou Zhu, Jinguo Zhu, Hao Li, Xiaoshi Wu, Xiaogang Wang, Hongsheng Li, Xiaohua Wang, and Jifeng Dai. 2021. Uni-Perceiver: Pre-training Unified Architecture for Generic Perception for Zero-shot and Few-shot Tasks. arXiv:2112.01522 [cs.CV]